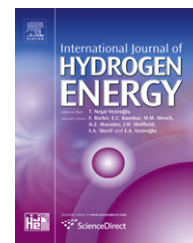


Available at www.sciencedirect.comjournal homepage: www.elsevier.com/locate/he

Analysis of heptane autothermal reformer to generate hydrogen for fuel cell applications

Chu Yan Nah, Srinivas Palanki*

Department of Chemical & Biomolecular Engineering, University of South Alabama, 307 University Blvd. N., Mobile, AL 36688-0002 USA

ARTICLE INFO

Article history:

Received 7 June 2009

Received in revised form

23 July 2009

Accepted 24 July 2009

Available online 1 September 2009

Keywords:

Heptane reformer

Hydrogen generation

ABSTRACT

In this paper, reaction engineering principles are utilized to analyze process conditions for producing sufficient hydrogen in a heptane autothermal reformer for generating 1 kW of power in a fuel cell. It is shown that operating the reformer adiabatically results in a sharp decrease in temperature due to endothermic reactions, which results in low conversion of heptane. For this reason, a heating jacket is added to the reformer where heptane is combusted to provide heat for the endothermic reactions. It is observed that when the reactor is operated non-isothermally, it is possible to get complete conversion of heptane and produce sufficient hydrogen to generate 1 kW of power via a fuel cell.

© 2009 Professor T. Nejat Veziroglu. Published by Elsevier Ltd. All rights reserved.

1. Introduction

Most urban areas have access to power via the electricity grid. However, in the battlefield or in remote campsites, batteries are the main energy source, but the acquisition, storage, distribution, and disposal of different types of battery poses an enormous challenge [16]. Fuel economy and emission abatement are critical issues in the automotive industry. Heavy duty trucks operate in idling mode for 20–40% of their operating time and utilize power during idling to operate comfort systems such as air conditioners, lights, radios and microwave ovens [12]. Both these scenarios provide the motivation for developing an auxiliary power system that utilizes a readily available hydrocarbon such as gasoline to generate power. Fuel cells have thermodynamic and environmental advantages over combustion-based processes for generating electricity [4]. Since fuel cells can use hydrogen as a fuel, there is renewed interest in technologies for producing hydrogen from hydrocarbon fuels, especially for small-scale power generation units up to 1 kW of power [10]. Power generators based on fuel cells offer advantages including high

efficiencies, low emissions, high reliability, quiet operation and easy monitoring when compared to conventional gasoline-powered generators [4].

Autothermal reforming of higher hydrocarbons such as gasoline is an attractive route for the production of hydrogen for use in the generation of power from fuel cells for stationary power applications [3]. In autothermal reforming, there are two different sets of reactions: (1) steam reforming of hydrocarbons and (2) oxidation of hydrocarbons. The oxidation reactions are exothermic while the steam reforming reactions are endothermic. Under the right set of conditions, the heat required for steam reforming can be generated by the oxidation reaction. In the literature, there are two different ways of operating a reformer under autothermal conditions: (1) the steam reforming reactions and the oxidation reaction occur in the same chamber [2] and (2) the steam reforming reactions and the oxidation reaction occur in different chambers and heat is transferred through a physical barrier [14]. In this paper, we consider the second option, primarily because this allows for a higher yield of hydrogen in the reactor [8].

* Corresponding author.

E-mail address: spalanki@usouthal.edu (S. Palanki).

0360-3199/\$ – see front matter © 2009 Professor T. Nejat Veziroglu. Published by Elsevier Ltd. All rights reserved.

doi:10.1016/j.ijhydene.2009.07.106

The development of reformers that provide hydrogen to power fuel cell stacks has been a subject of considerable research activity [7,5]. Kundu et al. [9] developed a serpentine patterned micro-reformer that converts methanol to hydrogen via steam reforming. Sohn et al. [21] developed a plate-type integrated fuel processor-PEM fuel cell where methanol is reformed to produce up to 150 W of power. Tan et al. [23] developed a methane processing system for producing high-purity hydrogen for 10 W–1500 W power applications. Lindstrom et al. [12] developed a diesel fuel reformer for generating hydrogen for an auxiliary power unit in a truck. In parallel with these experimental efforts, there has been considerable interest in developing kinetic models for the reforming of several different hydrocarbons. For instance, Xu and Froment [27] developed intrinsic rate expressions for the steam reforming of methane on a nickel catalyst. Kinetic expressions for methanol steam reforming on Cu/ZnO/Al₂O₃ catalyst were developed by Peppley et al. [18,19]. Tottrup [26] developed an intrinsic kinetic expression for heptane reforming on a nickel catalyst. Thormann et al. [24] developed kinetic expressions for steam reforming of hexadecane over a Rh/CeO₂ catalyst. While there is considerable literature on fabrication of reformers that demonstrate the feasibility of utilizing hydrocarbon fuel to produce hydrogen and kinetic expressions are available for a large number of model hydrocarbons, there are very few papers in modeling and analysis of these reactors, which is necessary for optimizing performance. In particular, the literature is very sparse in papers where reaction kinetics are utilized in conjunction with heat transfer calculations to determine the size and performance of reformers operating non-isothermally.

In this paper a packed bed reactor is analyzed in which autothermal reforming of heptane occurs to produce hydrogen. In particular, the reformer is modeled as a non-isothermal, non-isobaric packed bed reactor. Heat is supplied to the reactor via a jacket where heptane combustion occurs. The heat transfer coefficient between the jacket and the reactor is computed when heptane is combusted in the jacket and endothermic steam reforming of heptane occurs in the reactor. Reactor conditions are analyzed to generate sufficient hydrogen that can be used in a solid oxide fuel cell to produce 1 kW of power. A schematic of the process under consideration is shown in Fig. 1. Heptane is used as a model higher hydrocarbon. Kinetics of heptane steam reforming are available in the literature and it is expected that the results obtained would be similar to those of higher hydrocarbon mixtures such as gasoline [2].

2. Reaction kinetics of heptane reforming

Many researchers have used the following reactions to study steam reforming of heptane on nickel catalysts [3,2]:

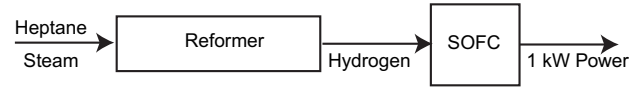


Fig. 1 – Schematic of reformer and fuel cell system.



The heptane reforming reaction, Eq. (1), is considered irreversible and C₁-components (methane and carbon oxides) are formed with no intermediates [3]. Methane, carbon monoxide and carbon dioxide are produced by methanation, Eqs. (2) and (3), and water–gas shift reaction, Eq. (4), respectively.

Tottrup [26] provided the following intrinsic kinetic expression for the heptane reforming reaction represented by Eq. (1):

$$r_{1,\text{C}_7\text{H}_{16}} = -\frac{k_1 P_{\text{C}_7\text{H}_{16}}}{\left[1 + K_A \frac{P_{\text{C}_7\text{H}_{16}} P_{\text{H}_2}}{P_{\text{H}_2\text{O}}} + K_B \frac{P_{\text{H}_2\text{O}}}{P_{\text{H}_2}}\right]^2} \quad (5)$$

where $r_{1,\text{C}_7\text{H}_{16}}$ is the reaction rate for steam reforming of heptane; $P_{\text{C}_7\text{H}_{16}}$, P_{H_2} and $P_{\text{H}_2\text{O}}$ are partial pressures of heptane, hydrogen and steam, respectively.

The reforming gas is rich in methane due to methanation reactions (2) and (3) and, therefore, steam reforming of methane takes place [2]. Xu and Froment [27] have provided the following kinetic expressions for steam reforming of methane:

$$\text{CH}_4 + \text{H}_2\text{O} \rightleftharpoons \text{CO} + 3\text{H}_2$$

$$r_{2,\text{CO}} = \frac{k_2 \left(P_{\text{CH}_4} P_{\text{H}_2\text{O}} - \frac{P_{\text{H}_2}^3 P_{\text{CO}}}{K_1} \right)}{\left(1 + K_{\text{CO}} P_{\text{CO}} + K_{\text{H}_2} P_{\text{H}_2} + K_{\text{CH}_4} P_{\text{CH}_4} + K_{\text{H}_2\text{O}} P_{\text{H}_2\text{O}} / P_{\text{H}_2}\right)^2} \quad (6)$$

$$\text{CO}_2 + \text{H}_2 \rightleftharpoons \text{CO} + \text{H}_2\text{O}$$

$$r_{3,\text{CO}_2} = \frac{k_3 \left(P_{\text{CO}} P_{\text{H}_2\text{O}} - \frac{P_{\text{H}_2} P_{\text{CO}_2}}{K_2} \right)}{\left(1 + K_{\text{CO}} P_{\text{CO}} + K_{\text{H}_2} P_{\text{H}_2} + K_{\text{CH}_4} P_{\text{CH}_4} + K_{\text{H}_2\text{O}} P_{\text{H}_2\text{O}} / P_{\text{H}_2}\right)^2} \quad (7)$$

$$\text{CH}_4 + 2\text{H}_2\text{O} \rightleftharpoons \text{CO}_2 + 4\text{H}_2$$

$$r_{4,\text{CO}_2} = \frac{k_4 \left(P_{\text{CH}_4} P_{\text{H}_2\text{O}}^2 - \frac{P_{\text{H}_2}^4 P_{\text{CO}_2}}{K_3} \right)}{\left(1 + K_{\text{CO}} P_{\text{CO}} + K_{\text{H}_2} P_{\text{H}_2} + K_{\text{CH}_4} P_{\text{CH}_4} + K_{\text{H}_2\text{O}} P_{\text{H}_2\text{O}} / P_{\text{H}_2}\right)^2} \quad (8)$$

where $r_{2,\text{CO}}$, r_{3,CO_2} , and r_{4,CO_2} , are rates of reaction for steam reforming of methane and water–gas shift reactions, and P_{CH_4} , P_{CO} , and P_{O_2} are the partial pressures of methane, carbon monoxide and carbon dioxide, respectively.

3. Reformer modeling and simulation conditions

The reformer is modeled as a jacketed packed bed tubular reactor with constant cross-sectional area, A_c . The steady-state model equations for each species are given as follows [6]:

$$\frac{dF_{\text{C}_7\text{H}_{16}}}{dz} = (r_{1,\text{C}_7\text{H}_{16}}) A_c \quad (9)$$

$$\frac{dF_{\text{H}_2\text{O}}}{dz} = (7r_{1,\text{C}_7\text{H}_{16}} - r_{2,\text{CO}} - r_{3,\text{CO}_2} - 2r_{4,\text{CO}_2}) A_c \quad (10)$$

$$\frac{dF_{CO}}{dz} = (-7r_{1,C_7H_{16}} + r_{2,CO} - r_{3,CO_2})A_c \quad (11)$$

$$\frac{dF_{H_2}}{dz} = (-15r_{1,C_7H_{16}} + 3r_{2,CO} + r_{3,CO_2} + 4r_{4,CO_2})A_c \quad (12)$$

$$\frac{dF_{CH_4}}{dz} = (-r_{2,CO} - r_{4,CO_2})A_c \quad (13)$$

$$\frac{dF_{CO_2}}{dz} = (r_{3,CO_2} + r_{4,CO_2})A_c \quad (14)$$

where $F_{C_7H_{16}}$, F_{H_2O} , F_{CO} , F_{H_2} , F_{CH_4} , and F_{CO_2} , are the molar flow rates of heptane, steam, carbon monoxide, hydrogen, methane, and carbon dioxide, respectively, z is the length dimension of the tubular reactor, $r_{1,C_7H_{16}}$ is the reaction rate for

from [20] and the collision integral is calculated by the following equation:

$$\Omega = \frac{a}{T^b} + \frac{c}{e^{\bar{T}d}} + \frac{e}{e^{\bar{T}f}} \quad (19)$$

where \bar{T} is the dimensionless temperature given by T/E_k and E_k is the minimum of pair potential energy divided by Boltzmann constant and a , b , c , d , and e are collision integral constants. Minimum of pair potential energy is obtained from Poling et al. [20]. Dimensionless temperature is used to determine the collision integral by means of collision integral constants.

A steady state energy balance on the reformer leads to the following equation [6]:

$$\frac{dT}{dz} = \frac{(UA\Delta T + r_{1,C_7H_{16}}\Delta H_1 + r_{2,CO}\Delta H_2 + r_{3,CO_2}\Delta H_3 + r_{4,CO_2}\Delta H_4)}{(F_{C_7H_{16}}C_{pC_7H_{16}} + F_{H_2O}C_{pH_2O} + F_{CO}C_{pCO} + F_{H_2}C_{pH_2} + F_{CH_4}C_{pCH_4} + F_{CO_2}C_{pCO_2})}A_c \quad (20)$$

steam reforming of heptane represented by Eq. (5), and $r_{2,CO}$, r_{3,CO_2} , r_{4,CO_2} , are rates of reaction for steam reforming of methane and water–gas shift reactions represented by Eqs. (6)–(8). The pressure drop is modeled via the Ergun Equation [6]:

$$\frac{dP}{dz} = -\frac{G}{\rho D_p} \left(\frac{1-\phi}{\phi^3} \right) \left[\frac{150(1-\phi)\eta_m}{D_p} + 1.75G \right] \quad (15)$$

where P is the reactor pressure, ϕ is the void fraction, D_p is the diameter of the catalyst particle in the reformer, η_m is the viscosity of the gas mixture, ρ is the gas mixture density and G is the superficial mass velocity.

The Ergun equation requires the computation of the gas mixture density, ρ , as well as the gas mixture viscosity, η_m , as a function of reactor length. The mixture density is estimated by computing the mole average density of the gas mixture at each integration step. Due to the presence of hydrogen in the gas mixture, the mole average method can lead to significant errors in the overall gas mixture viscosity [1]. For this reason, Wilke's method [20] is utilized to estimate the gas viscosity at each integration step as shown below:

$$\eta_m = \frac{\sum_{i=1}^n y_i \eta_i}{\sum_{j=1}^n y_j \phi_{ij}} \quad (16)$$

where

$$\phi_{ij} = \frac{\left[1 + \left(\frac{\eta_i}{\eta_j} \right)^{0.5} \left(\frac{M_i}{M_j} \right)^{0.25} \right]^2}{\left[8 \left(1 + \left(\frac{M_i}{M_j} \right) \right) \right]^{0.5}} \quad (17)$$

In the above equations η_m is the viscosity of the mixture, η_i , y_i , and M_i are the viscosity, mole fraction and molecular weight, respectively, of pure component i . The pure component viscosity is calculated by the following equation

$$\eta_i = \frac{(26.69MT)^{0.5}}{\sigma^2 \Omega} \quad (18)$$

where σ is the hard sphere diameter, Ω is the collision integral and T is the temperature. Hard sphere diameters are obtained

where T is the reformer temperature, ΔH_i is the heat of reaction for reaction r_i , U is the overall heat transfer coefficient between the jacket and the reactor, A is the heat transfer area, ΔT is the temperature difference between the jacket and the reactor at a length z , and C_{p_j} is the specific heat of species j .

The overall coefficient, U , is constructed from the individual coefficients and the resistance of the tube wall. The overall heat transfer coefficient is calculated by the following equation [13]:

$$U = \frac{1}{\frac{1}{h_i} \frac{D_o}{D_i} + \frac{x_w}{k_m} \left(\frac{D_o - D_i}{\ln \left(\frac{D_o}{D_i} \right)} \right) + \frac{1}{h_o}} \quad (21)$$

where D_o is the outer diameter of the tubular reactor, D_i is the inner diameter of the tubular reactor, h_o is the individual heat transfer coefficient at the annulus side of the reactor, h_i is the individual heat transfer coefficient for packed bed reactor side, x_w is the reactor wall thickness and k_m is the thermal conductivity of the reactor wall. The Sieder–Tale equation is used to estimate the individual heat transfer coefficient on the annulus side [13]:

$$h_o = J_H \frac{k_m}{D_o} \left(\frac{C_p \mu_m}{k_m} \right)^{\frac{1}{3}} \quad (22)$$

where J_H is the Colburn j factor, C_p is the average specific heat and μ_m is the mixture viscosity. To predict the rate of heat transfer on the reactor side for different particle and tube sizes, gas flow rates, and gas properties, the coefficient h_i is to account for the resistance in the region very near to the wall and for the resistance in the rest of the packed bed. This coefficient is estimated from the following empirical equation, which was determined by subtracting the calculated bed resistance from the measured overall resistance [25]:

$$h_i = \left(0.4Re_p^{\frac{1}{2}} + 0.2Re_p^{\frac{2}{3}} \right) Pr^{0.4} \frac{1-\phi}{\phi} \frac{k_{m_i}}{D_p} \quad (23)$$

Table 1 – Kinetic parameters.

Kinetic parameter	Value
k_1 (Specific reaction rate)	$3.906 \times 10^8 \exp(-67800/(RT))$ mol/ ($m^3 \cdot s \cdot atm$)
k_2 (Specific reaction rate)	$9.886 \times 10^{16} \exp(-240100/(RT))$ ($mol \cdot atm^{0.5} / (m^3 \cdot min)$)
k_3 (Specific reaction rate)	$4.665 \times 10^7 \exp(-67130/(RT))$ mol/ ($atm \cdot m^3 \cdot min$)
k_4 (Specific reaction rate)	$2.386 \times 10^{16} \exp(-243900/(RT))$ ($mol \cdot atm^{0.5} / (m^3 \cdot min)$)
K_A (Adsorption constant)	25.2 (atm^{-1})
K_B (Adsorption constant)	0.077
K_1 (Equilibrium constant)	$\exp(29.3014 - 26248.4/T)$
K_2 (Equilibrium constant)	$\exp(-4.35369 + 4593.17/T)$
K_3 (Equilibrium constant)	$\exp(25.225 - 21825.28/T)$
K_{CO} (Adsorption constant)	$8.339 \times 10^{-5} \exp(70650/(RT))$ (atm^{-1})
K_{H_2} (Adsorption constant)	$6.209 \times 10^{-9} \exp(82900/(RT))$ (atm^{-1})
K_{CH_4} (Adsorption constant)	$6.738 \times 10^{-4} \exp(38280/(RT))$ (atm^{-1})
K_{H_2O} (Dissociative constant)	$1.770 \times 10^5 \exp(-88680/(RT))$

where Re_p is the Reynold's number for the packed bed reactor, Pr is the Prandtl number, ϕ is the void fraction and k_{m_i} is the average thermal conductivity of the gas mixture. It was shown in [22] that diffusion effects for this reactor system are negligible and so all simulations done in this research assume that there are no diffusion effects.

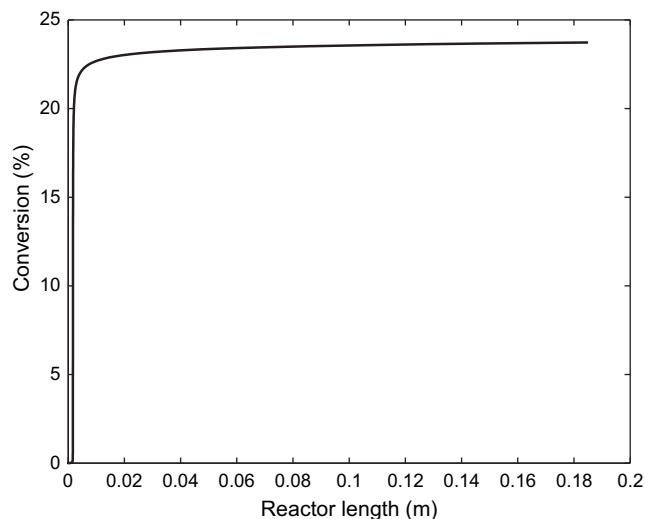
Tables 1 and 2 list the values of the kinetic parameters and reactor parameters used in simulation studies in this research.

4. Simulation results and discussion

The design equations described by Eqs. (9)–(15) were integrated numerically in MATLAB using the stiff ordinary

Table 2 – Reactor parameters.

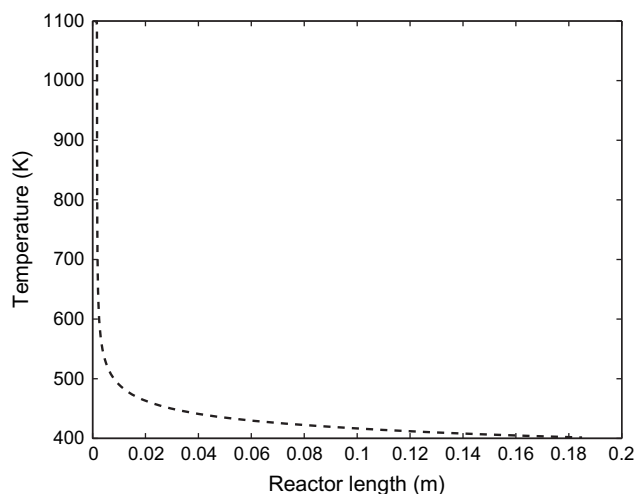
Reactor parameter	Value
Catalyst particle diameter, D_p	0.000186 m
Catalyst density, ρ	2835 kg/ m^3
Void fraction, ϕ	0.38
Reactor length, L	0.18 m
Reactor inner diameter, D_i	0.024 m
Reactor outer diameter, D_o	0.041 m

**Fig. 2 – Heptane conversion as a function of reactor length under adiabatic conditions.**

differential equations routine *ode15s*. The flow rate of heptane entering the reformer was set at 0.00075 mol/s. The effect of temperature, pressure, oxygen to heptane ratio and steam to heptane ratio on hydrogen production was analyzed by running simulations at a variety of process conditions as follows:

- Temperature range: 700–1100 K
- Steam to heptane ratio range: 7–20
- Inlet pressure range: 1–10 atm

The reaction kinetics developed in the literature are valid in the temperature, steam to heptane ratio and pressure range described above. It was determined in [15] that a hydrogen flow rate of 0.011 mol/s was necessary to generate 1 kW of power in a solid oxide fuel cell stack. The effect of changing process conditions to achieve this flow rate was studied.

**Fig. 3 – Temperature as a function of reactor length under adiabatic conditions.**

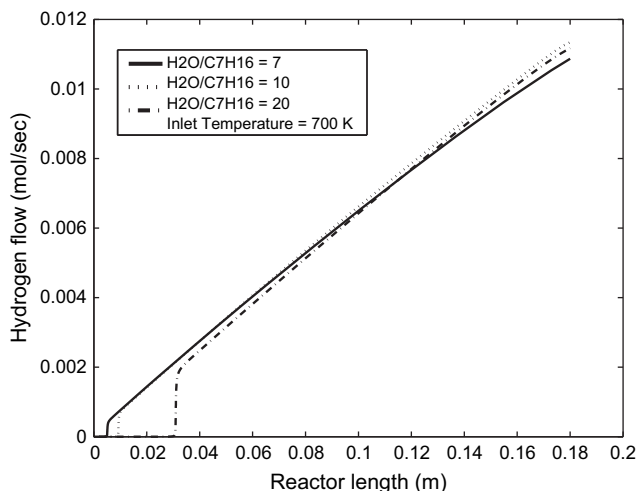


Fig. 4 – Effect of steam to heptane ratio on hydrogen production at an inlet temperature of 700 K.

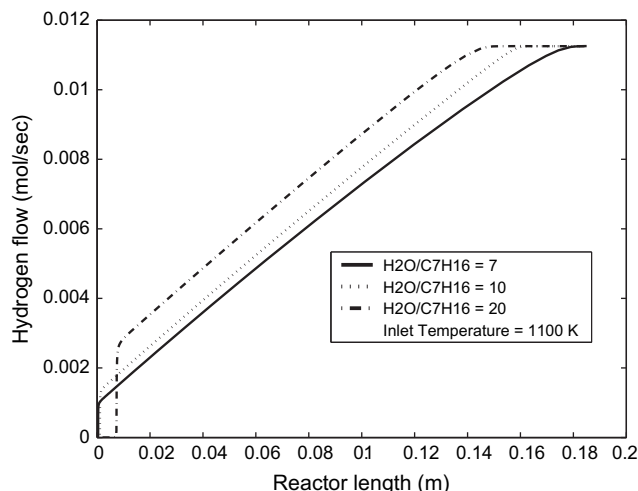


Fig. 6 – Effect of steam to heptane ratio on hydrogen production at an inlet temperature of 1100 K.

Initial simulations were conducted to study the effect of process conditions on hydrogen production when the reformer was operated adiabatically. Fig. 2 shows the plot of heptane conversion as a function of reactor length when the inlet temperature is 1100 K, steam to heptane ratio is 20 and the inlet pressure is 10 atm. It is observed that the conversion of heptane is low (<25%) and the amount of hydrogen produced is not sufficient to generate 1 kW of power. Beyond a reactor length of 0.04 m, conversion does not change since the temperature decreases below 450 K as shown in Fig. 3 and the reaction rate becomes almost zero. Decreasing the inlet pressure, inlet temperature and inlet steam to heptane ratio further decreases conversion (simulations not shown). This leads to the conclusion that adiabatic operation is impractical and it is necessary to provide an external source of heat.

Simulations were conducted assuming that there is a jacket around the reformer where heptane combustion occurs and provides heat to the reforming reactions in the

reformer. Using Eqs. (22) and (23), the average value of the overall heat transfer coefficient, U , was computed to be $45 \text{ W/m}^2\text{K}$. Using this overall heat transfer coefficient, the effect of changing inlet steam to heptane ratio, inlet pressure, and inlet temperature on the production of hydrogen was studied. Figs. 4–6 show the effect of changing the inlet steam to heptane ratio on hydrogen flow rate out of the reformer at three different inlet temperatures, 700 K, 900 K, and 1100 K, for the jacketed packed bed reactor. The inlet pressure is 2 atm for this set of simulations. For an inlet temperature of 700 K and a steam to heptane ratio of 7, the conversion of heptane is 98%. Complete conversion of heptane is observed when the steam to heptane ratio is increased to 20. At higher temperatures, it is observed that the hydrogen profile flattens out before the end of the reactor is reached, which indicates that heptane is completely converted and no more hydrogen is produced towards the end of the reactor. Thus, for a fixed reactor

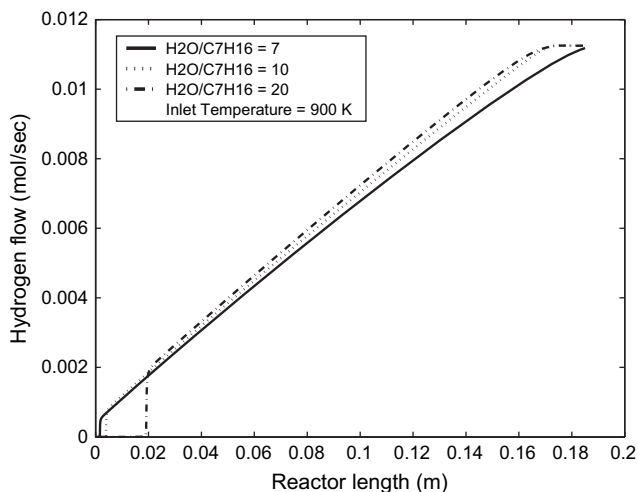


Fig. 5 – Effect of steam to heptane ratio on hydrogen production at an inlet temperature of 900 K.

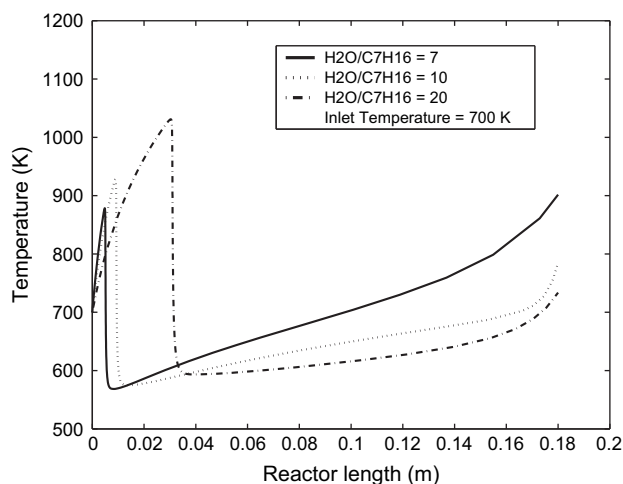


Fig. 7 – Temperature profile in reactor at an inlet temperature of 700 K.

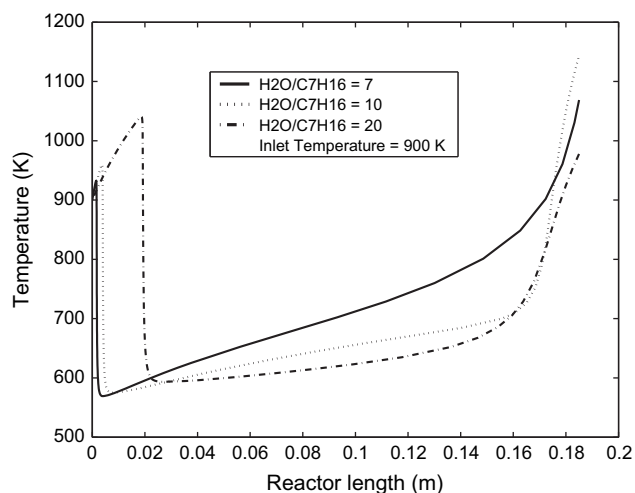


Fig. 8 – Temperature profile in reactor at an inlet temperature of 900 K.

length and fixed inlet heptane flow rate, hydrogen production can be increased by a combination of increasing temperature and increasing steam to heptane ratio. Figs. 7–9 show the corresponding temperature change along the reactor length with steam to heptane ratio on hydrogen flow rate out of the reformer for the conditions described for Figs. 4–6. It is observed that the temperature initially goes up and then decreases sharply when the endothermic reforming reactions start. The temperature along the length of the reactor then slowly increases due to the heat provided by the jacket. The reactor length at the point where the temperature drops dramatically increases with the inlet steam to heptane ratio, which indicates that large steam to heptane ratios tend to delay the onset of the endothermic reactions. When heptane is completely converted near the end of the reactor, the temperature goes up rapidly due to the absence of endothermic reactions. Fig. 10 shows the effect of changing inlet pressure on

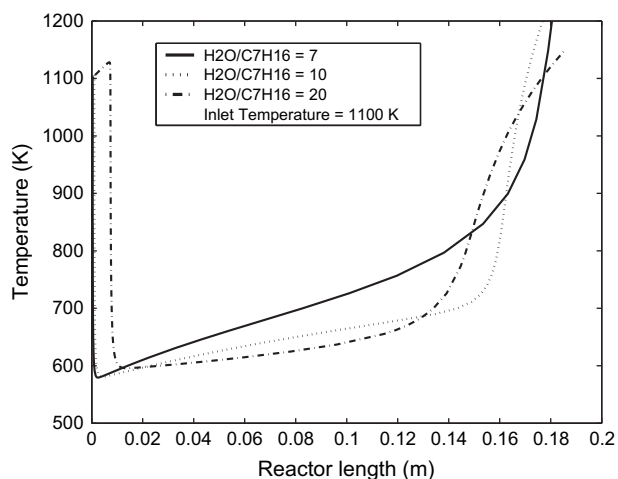


Fig. 9 – Temperature profile in reactor at an inlet temperature of 1100 K.

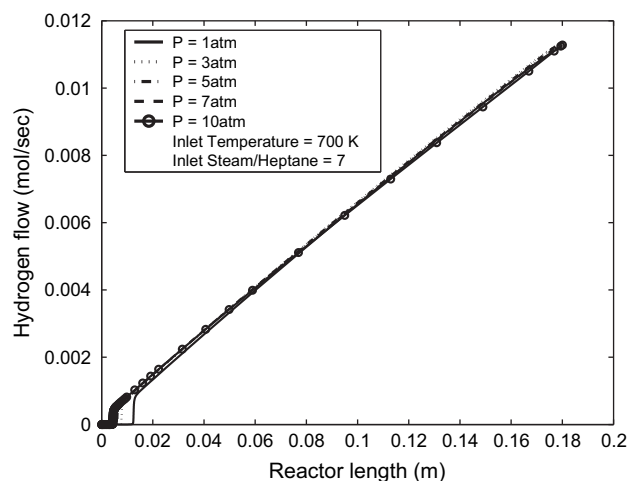


Fig. 10 – Effect of changing inlet pressure on hydrogen production.

hydrogen production at a steam to heptane ratio of 7 and an inlet temperature of 700 K. It is observed that the inlet pressure has a negligible effect on the hydrogen flow rate coming out of the reactor.

The above simulations indicate that it is feasible to produce the desired amount of hydrogen when the system is operated with a heating jacket. Further simulations were conducted assuming that the reformer feed was at 373 K while the jacket inlet temperature was at 2100 K to simulate practical experimental conditions. This implies that there is a vaporizer upstream of the reformer that converts liquid water and heptane to a vapor stream at 373 K similar to the experimental set-up reported by Lattner and Harold [11] for a methanol–water mixture. In this scenario, the reactant gases are heated from an initial temperature of 373 K in the reformer and an appreciable rate of reaction occurs only when the temperature goes over 600 K. Fig. 11 shows the flow rate of heptane, hydrogen and carbon

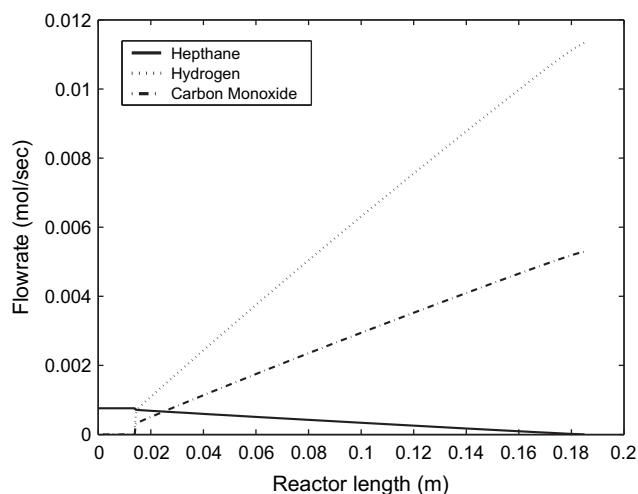


Fig. 11 – Flow rate of heptane, hydrogen and carbon monoxide under non-adiabatic operation.

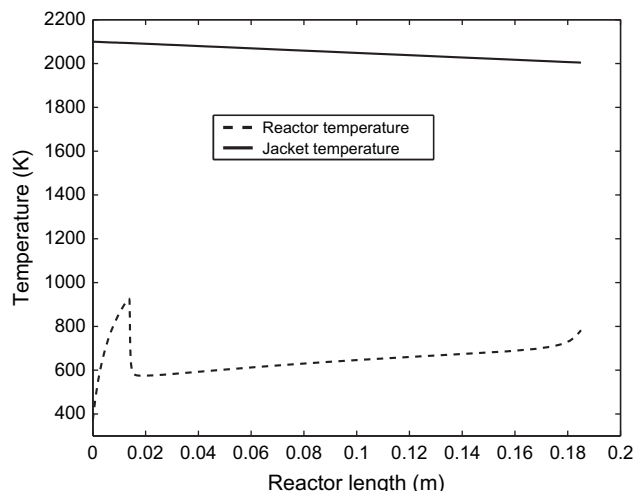


Fig. 12 – Reactor and jacket temperature as a function of reactor length.

monoxide along the reactor length at an inlet pressure of 2 atm and inlet steam to heptane ratio of 10. It is observed that for a heptane inlet flow rate 0.00075 mol/s, the hydrogen coming out of the reformer is 0.0113 mol/s, which is sufficient to produce 1 kW of power via a fuel cell. Fig. 12 shows the corresponding reactor and jacket temperature. Fig. 13 shows the corresponding pressure profile as a function of reactor length. The combustion of heptane in the jacket provides heat to the reformer. There is no appreciable reaction in the first 0.01 m of the reactor until the reformer temperature is above 600 K. Conversion is nearly 100% at the end of the reactor and the pressure drop is negligible. This indicates that the pressure drop due to fluid flow in the packed bed is balanced by the pressure elevation due to the substantial increase in the number of moles as the reaction proceeds along the length of the reformer. A large amount of carbon monoxide is produced along with the hydrogen.

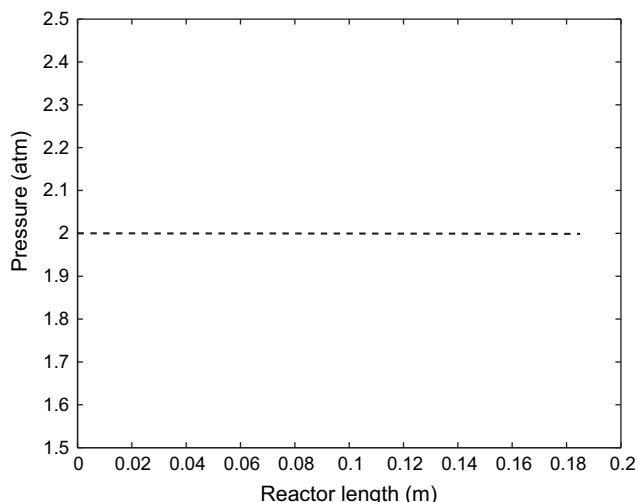


Fig. 13 – Reactor pressure as a function of reactor length.

5. Conclusions

In this paper, reaction engineering principles are utilized to analyze process conditions for producing sufficient hydrogen in a heptane autothermal reformer for generating 1 kW of power in a fuel cell. It is shown that operating the reformer adiabatically results in a sharp decrease in temperature due to endothermic reactions, which results in low conversion of heptane. For this reason, a heating jacket is added to the reformer where heptane is combusted to provide heat for the endothermic reactions. Pressure increase due to the increase in the number of moles in the reactor is balanced by pressure drop due to flow of fluid in the packed bed and the overall pressure drop is observed to be negligible. The effect of inlet pressure on the production of hydrogen is negligible. It is observed that when the reactor is operated with a heating jacket, it is possible to get complete conversion of heptane and produce sufficient hydrogen to generate 1 kW of power via a fuel cell. Given the large amount of carbon monoxide in the hydrogen stream, a solid oxide fuel cell (SOFC) stack is suggested for generating power. SOFCs use a solid ceramic inorganic oxide as the electrode (e.g., yttria-stabilized zirconia) and operate at elevated temperatures, typically between 750 and 1000 °C. They are tolerant to carbon monoxide and other impurities in the hydrogen stream [17]. The high quality heat generated by the fuel cell can be used to pre-heat the feed to the reformer, thereby increasing overall efficiency.

REFERENCES

- [1] Bird RB, Stewart LE, Lightfoot EN. Transport phenomena. 2nd ed. John Wiley and Sons; 2002.
- [2] Chen Z, Yan Y, Elnashaie SSEH. Modeling and optimization of a novel membrane reformer for higher hydrocarbons. *AIChE J* 2003;49(5):1250–65.
- [3] Christensen TS. Adiabatic prereforming of hydrocarbons—an important step in syngas production. *Appl Catal A Gen* 1996;138:285.
- [4] Cooper HW. Fuel cells, the hydrogen economy and you. *Chem Eng Progress* 2007;103(11):34–43.
- [5] deWild PJ, Verhaak MJFM. Catalytic production of hydrogen from methanol. *Catal Today* 2000;60(1):3–10.
- [6] Fogler HS. Elements of chemical reactor engineering. Upper Saddle River: Prentice-Hall; 2006.
- [7] Holladay JD, Jones EO, Phelps M, Hu J. Microfuel processor for use in a miniature power supply. *J Power Sources* 2002; 108:21.
- [8] Kaila RK, Krause AOI. Autothermal reforming of simulated gasoline and diesel fuels. *Int J Hydrogen Energy* 2006;31: 1934–41.
- [9] Kundu A, Jang JH, Gil JH, Jung CR, Lee HR, Kim SH, et al. Micro-fuel cells-current development and applications. *J Power Sources* 2007;170:67–78.
- [10] Larminie J, Dicks A. Fuel cell systems. New York: Wiley; 2000.
- [11] Lattner JR, Harold MP. Autothermal reforming of methanol: experiments and modeling. *Catal Today* 2007;120:78–89.
- [12] Lindstrom B, Karlsson JAJ, Ekdunge P, De Verdier L, Haggendal B, Dawody J, et al. Diesel fuel reformer for automotive fuel cell applications. *Int J Hydrogen Energy* 2009; 34:3367–81.

- [13] McCabe WL, Smith JC, Harriott P. Unit operations of chemical engineering. 6th ed. NY: McGraw-Hill Companies, Inc.; 2001.
- [14] Mu X, Pan L, Liu N, Zhang C, Li S, Sun G, et al. Autothermal reforming of methanol in a mini-reactor for a miniature fuel cell. *Int J Hydrogen Energy* 2007;32:3327–34.
- [15] Nah CY. Design and analysis of heptane autothermal reformer for fuel cell applications. Mobile, Alabama: University of South Alabama; 2008.
- [16] National Research Council. Meeting the energy needs of future warriors. Available at: <<http://www.nap.edu/catalog/11065.html>>; 2004 [accessed 15.01.09].
- [17] Ormerod RM. Solid oxide fuel cells. *Chem Soc Rev* 2003;32:17–28.
- [18] Peppley BA, Amphlett JC, Kearns LM, Mann RF. Methanol-steam reforming on Cu/ZnO/Al₂O₃ catalysts. Part 1. The reaction network. *Appl Catal A Gen* 1999a;179:21–9.
- [19] Peppley BA, Amphlett JC, Kearns LM, Mann RF. Methanol-steam reforming on Cu/ZnO/Al₂O₃ catalysts. Part 2. A comprehensive kinetic model. *Appl Catal A Gen* 1999b;179:31–49.
- [20] Poling BE, Prausnitz JM, O'Connell JP. The properties of gases and liquids. 5th ed. McGraw-Hill; 2001.
- [21] Sohn JM, Byun YC, Cho JY, Choe J, Song KH. Development of the integrated methanol fuel processor using micro-channel patterned devices and its performance for steam reforming of methanol. *Int J Hydrogen Energy* 2007;32: 5103–8.
- [22] Sukhavasi PV. Design and analysis of heptane reformer for hydrogen production for use in fuel cell applications. Mobile, Alabama: University of South Alabama; 2008.
- [23] Tan O, Masalaci E, Onsan ZI, Avci AK. Design of a methane processing system producing high-purity hydrogen. *Int J Hydrogen Energy* 2008;33:5516–26.
- [24] Thormann J, Maier L, Pfeifer P, Kunz U, Deutschmann O, Schubert K. Steam reforming of hexadecane over a Rh/CeO₂ catalyst in microchannels: experimental and numerical investigation. *Int J Hydrogen Energy* 2009;34: 5108–20.
- [25] Tosun I. Modeling in transport phenomena. 2nd ed. UK: Elsevier BV; 2007.
- [26] Tottrup PB. Evaluation of intrinsic steam reforming kinetic parameters from rate measurements on full particle size. *Appl Catal* 1982;4:377.
- [27] Xu JG, Froment GF. Methane steam reforming, methanation and water-gas shift .1. Intrinsic kinetics. *AIChE J* 1989;35(1): 88–96.